

OVEREXPRESSION OF GTP CYCLOHYDROLASE 1 FEEDBACK REGULATORY PROTEIN IS PROTECTIVE IN A MURINE MODEL OF SEPTIC SHOCK

Anna Starr,* Claire A. Sand,* Lamia Heikal,* Peter D. Kelly,[†] Domenico Spina,* Mark Crabtree,[‡] Keith M. Channon,[‡] James M. Leiper,[†] and Manasi Nandi*

*Pharmacology and Therapeutics Group, Institute of Pharmaceutical Science, School of Biomedical Sciences, King's College London; and [†]MRC Clinical Sciences Centre, Faculty of Medicine, Imperial College London, London; and [‡]British Heart Foundation Centre of Research Excellence, Division of Cardiovascular Medicine, University of Oxford, John Radcliffe Hospital, Oxford, United Kingdom

Received 19 May 2014; first review completed 4 Jun 2014; accepted in final form 10 Jul 2014

ABSTRACT—Overproduction of nitric oxide (NO) by inducible NO synthase contributes toward refractory hypotension, impaired microvascular perfusion, and end-organ damage in septic shock patients. Tetrahydrobiopterin (BH₄) is an essential NOS cofactor. GTP cyclohydrolase 1 (GCH1) is the rate-limiting enzyme for BH₄ biosynthesis. Under inflammatory conditions, GCH1 activity and hence BH₄ levels are increased, supporting pathological NOS activity. GCH1 activity can be controlled through allosteric interactions with GCH1 feedback regulatory protein (GFRP). We investigated whether overexpression of GFRP can regulate BH₄ and NO production and attenuate cardiovascular dysfunction in sepsis. Sepsis was induced in mice conditionally overexpressing GFRP and wild-type littermates by cecal ligation and puncture. Blood pressure was monitored by radiotelemetry, and mesenteric blood flow was quantified by laser speckle contrast imaging. Blood biochemistry data were obtained using an iSTAT analyzer, and BH₄ levels were measured in plasma and tissues by high-performance liquid chromatography. Increased BH₄ and NO production and hypotension were observed in all mice, but the extents of these pathophysiological changes were attenuated in GFRP OE mice. Perturbations in blood biochemistry were similarly attenuated in GFRP OE compared with wild-type controls. These results suggest that GFRP overexpression regulates GCH1 activity during septic shock, which in turn limits BH₄ bioavailability for iNOS. We conclude that the GCH1-GFRP axis is a critical regulator of BH₄ and NO production and the cardiovascular derangements that occur in septic shock.

KEYWORDS—Tetrahydrobiopterin, vascular nitric oxide, circulatory shock, microvascular flow, sepsis

ABBREVIATIONS—GCH1 — GTP cyclohydrolase 1; GFRP — GCH1 feedback regulatory protein; BH₄ — tetrahydrobiopterin; CLP — cecal ligation and puncture

INTRODUCTION

There is a large unmet clinical need for novel therapies that can stabilize the cardiovascular system and reduce the requirement for vasopressor and inotropic support in septic shock patients (1). It is known that overproduction of nitric oxide (NO) contributes to the cardiovascular derangements observed in septic shock (2, 3). The three NO synthase (NOS) isoforms, endothelial, neuronal, and inducible (iNOS), each require the essential cofactor 6,R-L-5,6,7,8-tetrahydrobiopterin (BH₄), for full catalytic activity (4), and of the three isoforms, iNOS is believed to contribute most toward pathological in-

flammation and cardiovascular dysfunction in sepsis. BH₄ is synthesized from GTP in a three-step reaction in which the committing step is mediated by the enzyme GTP cyclohydrolase 1 (GCH1) (5). Modulation of GCH1 and BH₄ has been shown to regulate NO production and vascular function (6–9).

Under inflammatory conditions, expression and activity of GCH1 are increased, leading to a concomitant elevation in BH₄ levels; this is an absolute requirement to support iNOS activity (10–12). A greater understanding of this pathway could undoubtedly facilitate the development of novel strategies to limit pathological NO production in sepsis and inflammation. Indeed, some progress has been made in this area: both a pterin site inhibitor for NOS (4-amino tetrahydrobiopterin) and a GCH1 inhibitor (2,4-diamino-6-hydroxy-pyrimidine) have been shown to improve outcome in rodent models of sepsis (13, 14). However, such approaches, which entirely block BH₄ bioavailability for all three NOS isoforms, may lead to an “uncoupled” NOS enzyme, which itself could perpetuate vascular dysfunction through the generation of reactive oxygen species (15). Thus, reversible attenuation, rather than complete blockade, of BH₄ bioavailability for iNOS may be therapeutically advantageous.

Interestingly, mammals already have an endogenous method of reversibly controlling BH₄ bioavailability: GCH1 activity can be directly inhibited by BH₄, but only when GCH1 is complexed with its regulatory protein GFRP (GCH1 feedback

Address reprint requests to Manasi Nandi, PhD, Pharmacology and Therapeutics Group, Institute of Pharmaceutical Science, School of Biomedical Sciences, King's College London, Franklin-Wilkins Bldg, 150 Stamford St, London, United Kingdom SE1 9NH. E-mail: manasi.nandi@kcl.ac.uk.

Author Contributions: A.S. and M.N. conceived and designed the study; compiled, analyzed, and interpreted the data; and drafted the manuscript. C.A.S. and L.H. collected, analyzed, and interpreted blood flow and nitrite data, respectively. M.C. and K.M.C. provided access and training to the BH₄ detection system and interpretation of BH₄ data. D.S. performed the statistical analysis. J.M.L. and P.D.K. designed the transgenic mouse construct. All authors read and approved the final manuscript.

This work has been supported by The British Heart Foundation PG/09/073.

The authors declare they have no competing interests.

Supplemental digital content is available for this article. Direct URL citation appears in the printed text and is provided in the HTML and PDF versions of this article on the journal's Web site (www.shockjournal.com).

DOI: 10.1097/SHK.0000000000000235

Copyright © 2014 by the Shock Society

regulatory protein) (16). In other words, when BH₄ is produced in excess, it can switch off its own production by binding to selective pockets at the interface of the GCH1 and GFRP protein complex, inducing allosteric changes within GCH1, and limiting further BH₄ biosynthesis (16, 17). This allosteric negative feedback regulation is reversible and noncompetitive, and the BH₄ binding sites are distinct from the substrate (GTP) binding pockets (16, 17).

Furthermore, whereas GCH1 activity is markedly enhanced by proinflammatory stimuli, GFRP expression does not alter in the same manner (18, 19). Thus, under inflammatory conditions, there is a greater prevalence of unbound GCH1 protein, which would be insensitive to feedback inhibition by accumulating BH₄; this leads to maximal BH₄ bioavailability, which supports iNOS activity, perpetuating the inflammatory response. In support of this, we have previously demonstrated, *in vitro*, that endothelial GFRP overexpression significantly reduces BH₄ and NO generation following proinflammatory stimulation but has no effect on BH₄ or NO accumulation under naive conditions (20).

The present study aimed to build upon this work and establish whether altering the ratio of GFRP to GCH1 (through transgenic overexpression) could regulate BH₄ and NO *in vivo*. We hypothesized that overexpression of GFRP should maintain allosteric regulatory control of GCH1, limit the rise in BH₄ and NO that occurs under inflammatory conditions, and therefore be protective in sepsis. The current study evaluated the effect of overexpression of GFRP on cardiovascular hemodynamics, microvascular perfusion, and blood biochemistry in a murine model of septic shock.

METHODS

Experimental animals

All of the studies were conducted under a licence following King's College London ethics approval and in accordance with the UK Home Office Animals (Scientific Procedures) Act of 1986, under which humane end points must always be used, and hence mortality studies are not permitted.

Mice overexpressing GFRP were developed in collaboration with Nucleis (France). Briefly, murine GFRP cDNA was amplified by reverse transcriptase–polymerase chain reaction from mouse liver polyA + mRNA (AMS Biotechnology) with primers encoding a 5' *AccI* and 3' *NotI* restriction site. The polymerase chain reaction product was purified and digested with *AccI/NotI* and cloned downstream of a *Lox-Stop-Lox* cassette (provided by Nucleis in pBS302) in a pCI-Neo backbone vector. The GFRP expression cassette was transferred to pDEST (to create pDEST-GFRP). Following sequence verification, pDEST-GFRP was transfected into BPES embryonic stem cells. Homologous recombination of pDEST-GFRP into the modified HPRT locus of BPES cells reconstitutes HPRT activity rendering the cells resistant to hypoxanthine-aminopterin-thymidine (HAT medium) selection.

Recombinant BPES cells were injected into blastocysts, which were implanted into pseudopregnant mice. Chimeric male mice were identified by coat color and crossed to wild-type (WT) C57BL/6 females to establish germline transmission. Female offspring were then genotyped to confirm transgenesis. Transgenic female mice were crossed with pure C57BL/6 mice for more than 10 generations to obtain both male and female mice containing a dormant GFRP transgene on a pure C57BL/6 background. To activate expression of the transgene, female mice carrying the dormant transgene were crossed with C57BL/6 male mice expressing Cre recombinase under the control of the α smooth muscle actin promoter (α SM-Cre) (obtained by MTA originally from the laboratory of Dr Masashi Yanagisawa, UT Southwestern). Subsequently, male offspring obtained from the GFRP \times α SM-Cre cross were used for *in vivo* phenotyping studies. Mice with an excised *Lox-stop-Lox* codon (GFRP OE) were produced in the expected Mendelian frequencies, weaned, and housed with littermate controls expressing a dormant transgene (WT).

Male GFRP OE and WT mice, between 12 and 18 weeks of age, were used for all studies and group-housed with 12-h light-dark cycle and controlled

temperature of 20°C to 22°C. The mice were given free access to a normal chow diet and water *ad libitum*.

Appropriate sample size calculations were undertaken prior to experimentation based on published (21) and in-house pilot data, and investigators were blinded to genotype for all animal studies and unblinded after completion of data acquisition and analysis (22).

Western blot analysis

Tissue samples were homogenized, and cells were freeze-thawed in lysis buffer (Tris 50 mM, NaOH 150 mM, 1% Triton X; pH 7.4), including protease inhibitors (Roche Applied Science). Western blotting was carried out using standard techniques with mouse GFRP antibody (1:1,000 dilution; 200 μ g/mL, SC-22697; Santa Cruz Biotechnology, Santa Cruz, Calif), anti-goat immunoglobulin G–horseradish peroxidase (1:2,000 dilution; 200 μ g/mL, SC-2020; Santa Cruz Biotechnology), dilution GAPDH antibody (1:10,000; 1 mg/mL, MAB374; Millipore), and anti-mouse immunoglobulin G–horseradish peroxidase (1:2,000 dilution; 1 mg/mL, W402B; Millipore).

Implantation of radiotelemeters and hemodynamics measurements

PAC10 radiotelemetry devices (DSI) were implanted in 10- to 12-week-old mice under isoflurane anesthesia (2% through an air pump). Mice were maintained on a homeothermic heating blanket (Harvard Instruments) and eyes protected with Viscotears. The surgical field was sterilized with chlorhexidine, and buprenorphine hydrochloride (15 μ g/kg *i.m.*) was administered to provide analgesia. Telemeter catheters were advanced into the left carotid artery, with the body of the radiotransmitter placed in a subcutaneous pocket equidistant between the fore paw and hind paw. The incision was then closed with 5.0 Vicryl, and 40 mL/kg 0.9% saline resuscitation was given. Postoperatively, mice were held in a recovery cabinet at 27°C for 4 h and subsequently moved to a holding room. All mice underwent at least 10 days postoperative recovery before commencement of measurements. Blood pressure traces were checked, and animals with significant damping or loss of the hemodynamic signals were excluded from analysis in a blinded manner.

Radiotelemetry devices allow remote continuous monitoring of blood pressure, heart rate, and locomotor activity. Data were acquired continuously at 500 Hz using standard acquisition software (DSI). Baseline recording was carried out and averaged from six 24-h periods.

Evaluation of cardiac performance by echocardiography

Mice were anesthetized using inhaled isoflurane, chest hair removed with a topical depilatory agent, and mice were placed on a homeothermically heated table. Limb leads were attached for electrocardiogram gating, and mice were imaged in the left lateral decubitus position with a 30-MHz linear probe (30 MHz linear signal transducer; Visualsonic Vevo 770). Two-dimensional images in parasternal long- and short-axis projections were recorded with guided M-mode recordings at the midventricular level in both views. Interventricular septal and LV posterior wall dimensions were taken in diastole and systole, in addition to LV internal dimensions.

Cecal ligation and puncture

Following baseline hemodynamic recordings, polymicrobial sepsis was induced in the same telemetered mice by cecal ligation and puncture (CLP) as described previously (23). This method was chosen to incorporate the bacterial opsonization steps and more closely mimic the time course and pathology of clinical abdominal peritonitis. After laparotomy, the cecum was ligated distal to the ileocecal valve (bowel continuity preserved), punctured once through-and-through with a 19-gauge needle to express cecal content and returned to the peritoneal cavity. For sham operations, laparotomy was performed, but ligation and puncture omitted (23). After the procedure, 40 mL/kg 0.9% saline resuscitation was given subcutaneously. Continuous hemodynamic recording was started immediately; however, unlike baseline recordings, the room temperature was increased to 24°C. Mice were exsanguinated under terminal anesthesia (isoflurane) at 6 and 24 h (in accord with Home Office requirements), and plasma and tissue samples were collected and snap frozen immediately.

Evaluation of mesenteric blood flow by laser speckle contrast imaging

In a separate series of experiments, microcirculatory perfusion of the mesenteric bed was visualized and quantified using a MoorFLPI full-field laser perfusion imaging system and review software (Moor Instruments, Devon, UK), in CLP or sham GFRP OE and WT littermates after 6 or 24 h. Briefly, mice were anesthetized with 1.8% isoflurane on an air pump, and temperature was recorded and controlled by a homeothermic blanket. A section of the small intestine was exteriorized and pinned onto parafilm through the gut wall. Mice with excessive bleeding were immediately terminated and excluded from the study (<5% in our

studies). Vessels were moistened with saline (0.5 mL aerosolized) prewarmed to 37°C. The following acquisition modes and settings were used: high-resolution capture (100 frames; 4 s/frame); exposure 20 ms; automatic gain; flux palette set at 0 to 5,000, with background threshold 60 flux units.

Regions of interest were randomly selected and defined in equal number around first-, second-, and third-order descendants of the superior mesenteric artery, in which flux over time was analyzed offline by MoorFLPI review v.3 image analysis.

BH₄ measurement

BH₄ was measured from snap frozen tissue samples by electrochemical (Coulchem III; ESA Inc) detection following sample separation by high-performance liquid chromatography (HPLC) (24). High-performance liquid chromatography separation was performed using a 250-mm, ACE C-18 column (Hichrom) and a mobile phase comprising 50 mM sodium acetate, 5 mM citric acid, 48 μM EDTA, and 160 μM dithioerythritol (pH 5.2) at a flow rate of 1.3 mL/min. Background currents of +500 and -50 nA were used for the detection of BH₄ on electrochemical cells E1 and E2, respectively. Quantification of BH₄ was performed by comparison with external standards after normalizing for sample protein content.

Nitrite measurements

Plasma or tissue homogenates were deproteinated, and the nitrite content was then quantified using a fluorometric method utilizing 2,3-diaminonaphthalene. The amount of nitrite in each sample, expressed as μM nitrite/mg protein, was calculated from a linear calibration curve of known nitrite concentrations (linear range, 0.5–5 μM) and normalized for total amount of protein (in mg).

Blood biochemistry

Blood gases, biochemistry, and hematocrit were measured using an iSTAT Point-of-Care analyzer and EC8+ and Crea cartridges within 5 min of collection from the caudal vena cava (Abbott Laboratories, Princeton, NJ; Quality Clinical Reagents, UK). The lower limit of detection of the creatinine cartridges was 18 μmol/L.

Statistical analysis

Data are expressed as mean ± SEM or confidence intervals (mean ± error) from *n* mice. A mixed (fixed and repeated) analysis-of-variance approach was considered to analyze the hemodynamic data; however, because the variables conformed to diurnal variation, nonlinear regression was undertaken to fit the data to this well-described relationship.

For baseline hemodynamic data, a single sine model was used to fit a data set including all observations from all mice. Time was expressed as a fraction of 24 h and converted to a fraction of 2* π in order to fit the data to a sine wave. Diurnal variation can be represented as a sine wave and expressed as follows (25):

$$\text{cardiovascular variable} = \text{beta0} + \text{b0} + \text{beta1} * \left(\sin \left(2 * \pi / 24 * \text{time} \right) + \text{beta2} \right),$$

where beta0 represents the mean value for the cardiovascular variable, b0 is a random component that allows the mean to vary among mice, beta1 is an estimate of the amplitude, and beta2 is an offset that determines the location of the peak of the sine wave with respect to 9:00 h. A random effect for mice was included in the model because cardiovascular variables for a mouse were assumed to vary diurnally around that mouse's average (25).

In view of the downward trajectory of the cardiovascular parameters following CLP, an exponential function was also used; hence, the model was

described as $\text{beta0} + \text{b0} + (\text{beta1} * \exp(-\text{time} * \text{beta2}) * \sin[(2 * \pi / 24 * \text{time}) + \text{beta3}])$, where beta2 represented a time constant (*k*). The data were analyzed using the nonlinear mixed-model procedure of SAS (version 9.3) software for comparisons between parameters beta0 and *k*, and GraphPad Prism 4.0 software was used for graphical presentation of the data.

For other data sets, one-way analysis of variance and Bonferroni post test were performed using GraphPad Prism 4.0 software. Results were considered statistically significant when *P* < 0.05.

RESULTS

Characterization of GFRP OE mice

GFRP OE mice developed and bred normally and were indistinguishable from WT littermates. Multiple tissue samples obtained from mice expressing the GFRP transgene under the control of the α SM-Cre promoter demonstrated clear overexpression in the heart and skeletal muscle, but not in the liver (Fig. 1A). Semiquantitative densitometric analysis of autoradiograms obtained from Western blots revealed that GFRP was overexpressed between ~20- to 100-fold in the heart and skeletal muscle compared with ~1.5- to 3-fold increase in liver and lung. This tissue expression profile concurs with published studies using the α SM-Cre promoter (26). As previously reported, GFRP was highly expressed in liver samples from all mice (27), but there was no difference between WT and GFRP OE mice. Biochemical analysis revealed that BH₄ and nitrite levels were similar between GFRP OE and WT mice under basal conditions (Fig. 1, B and C).

Cardiovascular hemodynamics, basal and 24 h after CLP

Systolic and diastolic pressures and heart rate followed a normal diurnal pattern, and there was no significant difference between WT and GFRP OE groups under basal (naive) conditions (Fig. 2, A–C, left-hand side). Wild-type and GFRP OE mice also displayed normal diurnal changes in locomotor activity (high during hours of darkness) under naive conditions (Fig. 2D, left-hand side). Similar basal cardiac output (WT, 24.5 ± 1.4 mL/min; GFRP OE, 24.5 ± 1.5 mL/min) and ejection fraction (WT, 58% ± 3%; GFRP OE, 61% ± 3%) were also observed between the genotypes.

Subsequent induction of sepsis by CLP caused a time-dependent change in hemodynamic parameters, and locomotor activity was absent over a 24-h period; the shape of the time curve no longer followed a diurnal pattern (Fig. 2, A–C, right-hand side).

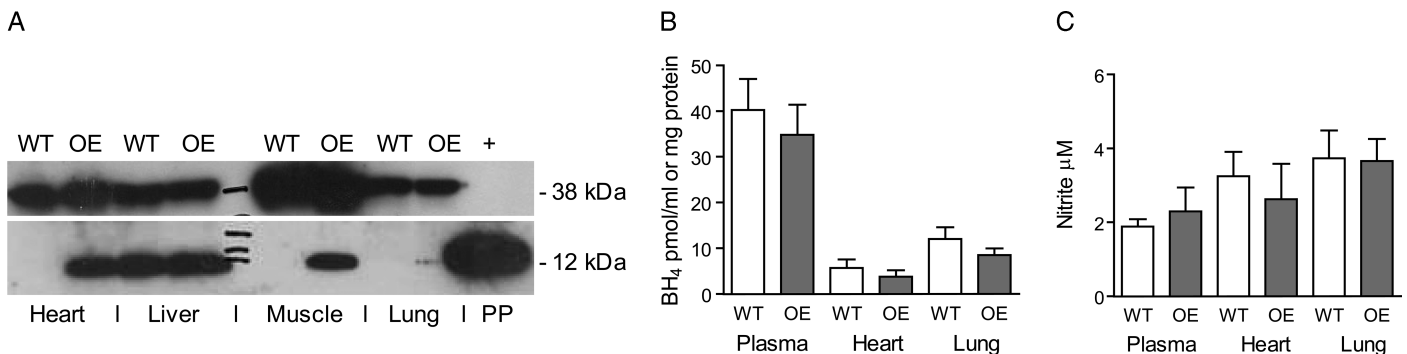


FIG. 1. **Characterization of GFRP-overexpressing animals.** A, Immunoblotting with mouse GFRP monoclonal antibody to detect overexpression GFRP protein identified a ~10 to 12-kd band in lysates from heart, liver, skeletal muscle, and lung. GAPDH (~40 kd) was used as a loading control and purified GFRP protein as a positive control. B, Plasma and tissue BH₄ levels, measured by HPLC, in naive untreated mice (mean ± SEM, *n* = 5). C, Fluorometric analysis of plasma and tissue nitrite levels in naive untreated mice (mean ± SEM, *n* = 5–6).

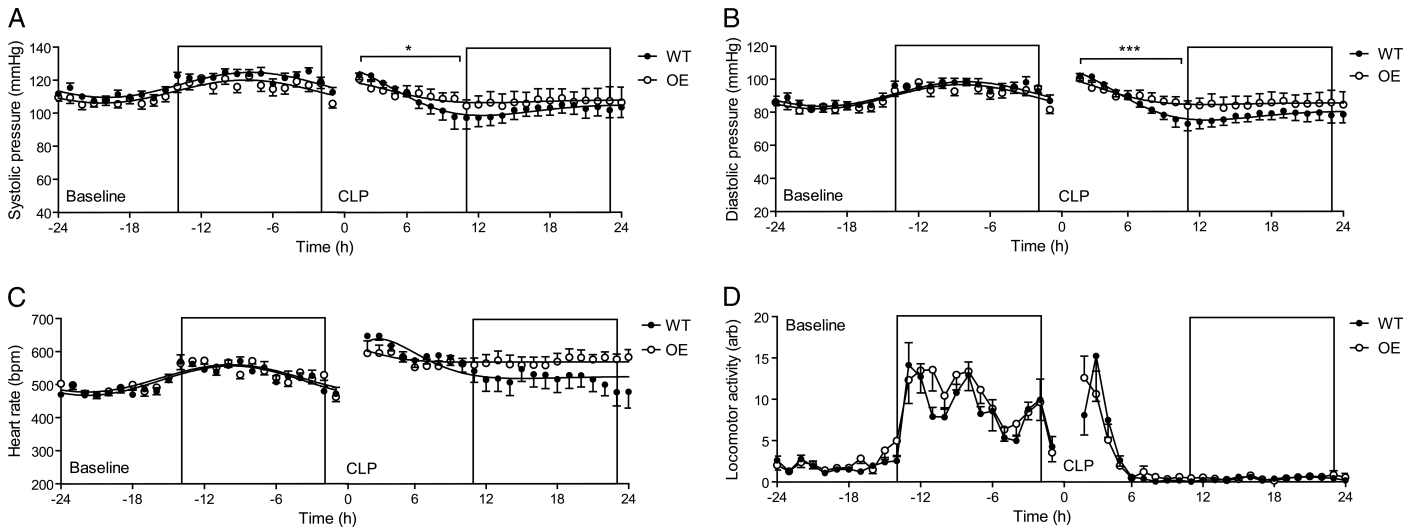


FIG. 2. **Cardiovascular hemodynamics in GFRP-overexpressing mice.** Systolic pressure (A), diastolic pressure (B), heart rate (C), and locomotor (D) activity of untreated WT and GFRP OE mice, recorded by radiotelemetry in undisturbed, singly housed, conscious animals. Hours of darkness are indicated by boxed section. Baseline values (left-hand side) are an average of six 24-h recording periods. Post-CLP recordings are taken over 24 h (right-hand side; mean \pm SEM, WT $n = 11$ or OE $n = 8$). The difference between the time constant, k , was 0.202 ± 0.09 for systolic pressure $*P = 0.0334$ and 0.228 ± 0.07 , $***P = 0.0048$ for diastolic pressure between WT and GFRP OE mice.

After CLP, systolic pressures recorded from WT mice initially rose compared with their paired time-matched naive values and then rapidly declined over 10 h (from 124 to 98 mmHg). In contrast, GFRP OE mice displayed a different profile, with a less pronounced and less rapid rate of decline in systolic pressure over 10 h (122 to 105 mmHg); pressure in these mice remained elevated compared with WT counterparts for the duration of the study (Fig. 2A, right-hand side). The same patterns were observed for diastolic blood pressure. There was a statistically significant difference in the rate (time constant, k) of developed hypotension in WT and GFRP OE groups for both systolic and diastolic pressure ($P < 0.01$; Figs. 2, A and B, right-hand side).

As with blood pressure, heart rate was similar between WT and GFRP OE mice under basal conditions (Fig 2C; left-hand side). However, tachycardia ($\sim 30\%$ increase) was observed after CLP treatment in all mice compared with the paired time-equivalent presepsis HR (Fig. 2C; right-hand side). Over the 24-h recording period after CLP, heart rate declined in WT mice (from 652 to 480 beats/min), whereas it remained elevated for in GFRP OE mice (from 603 to 556 beats/min). Furthermore, cardiac output fell in septic WT mice to 17.7 ± 1.7 mL/min ($n = 12$, $P < 0.01$ compared with baseline) and also in GFRP OE mice to 18.1 ± 1.1 mL/min ($n = 9$, $P < 0.05$ compared with baseline), whereas ejection fraction remained comparable to baseline values (WT $55\% \pm 4\%$, GFRP OE $62\% \pm 4\%$).

Mesenteric blood flow and metabolic disturbances after CLP

The mesenteric vasculature is an important vascular resistance bed in septic shock, and impaired flow in these vessels is known to correlate strongly with multiple organ failure and death (28). Assessment of mesenteric blood flow was performed *in situ* under isoflurane anesthesia. The small intestine was carefully pinned out to expose the mesenteric vasculature, and red blood cell flux was measured quantitatively and in real time across the entire portion of the exposed mesenteric vascular bed using laser speckle contrast imaging (Moor In-

struments). Laser speckle contrast imaging utilizes the random speckle patterns produced when tissue is illuminated by laser light. Automated processing of the contrast images generates real-time, high-resolution, color-coded flux images, which correlate with blood flow in each region.

Blood flow, quantified by this method, was severely impaired in mesenteric vessels of all mice following CLP by 24 h (Figs. 3, A and B), but no significant differences were detected between the GFRP OE and WT mice under naive or postseptic conditions.

However, despite similar impairments in mesenteric perfusion after CLP, analysis of blood biochemistry revealed that although WT mice displayed significant acidosis and impaired renal function (raised urea and creatinine) at 24 h, metabolic and renal function were not compromised to the same extent in GFRP OE mice (Figs. 3, C–E). Wild-type and GFRP OE mice also displayed similar body temperatures basally, but WT mice became significantly more hypothermic than GFRP OE mice following CLP (Fig. 3F). All other blood biochemistry data are summarized in Table, Supplemental Digital Content 1, at <http://links.lww.com/SHK/A223>. Notably, mice became severely hypoglycemic over the 24-h time period, consistent with previous reports (29, 30).

BH₄ and NO levels

Consistent with naive conditions, BH₄ and nitrite levels were similar between WT and GFRP OE mice following sham surgery (Fig. 4, A–D). BH₄ levels changed during sepsis progression in WT mice, rising significantly at 6 h and returning to baseline by 24 h, whereas mice overexpressing GFRP did not display this transient increase in BH₄ (Fig. 4, A and B).

A statistically significant increase in nitrite levels was observed in heart tissue after 24 h in WT mice but not in GFRP OE mice (Fig. 4C). Plasma nitrite remained unchanged in both groups of mice throughout (Fig. 4D).

Consistent with observations *in vitro* (18), we observed a reduction in GFRP protein expression in all mouse hearts 24 h

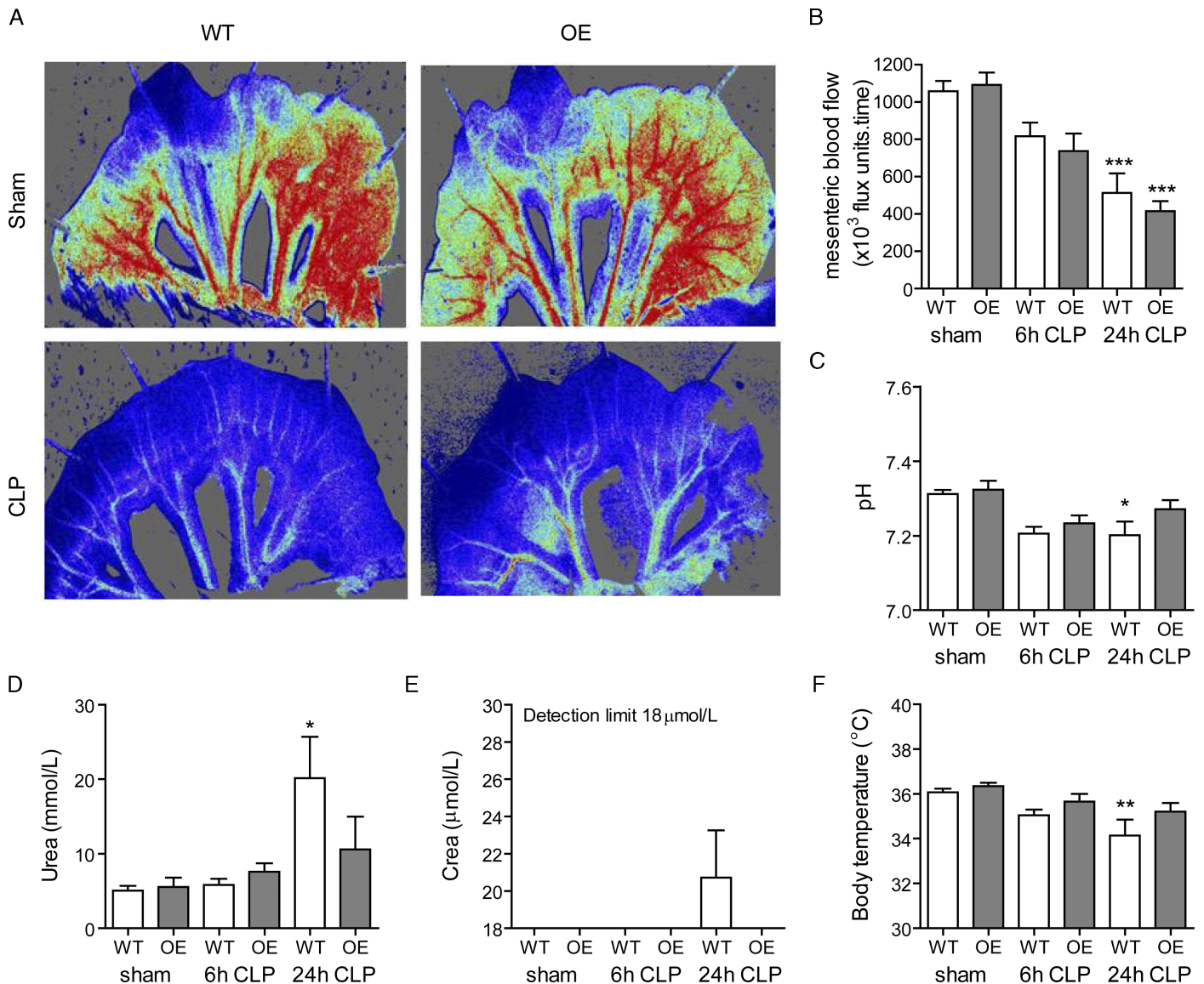


FIG. 3. **Microvascular and metabolic function in septic GFRP-overexpressing mice.** Assessment of mesenteric blood flow by laser speckle contrast imaging. A, Representative flux images taken during baseline recording and 24 h after CLP, red indicating areas of high flux, blue indicating areas of low flux. B, Total area under the flux curve over 5 m baseline recording period in sham and 6 and 24 h CLP-treated WT and GFRP OE mice ($n = 6-8$, mean \pm SEM, *** $P < 0.001$ compared with sham). (mean \pm SEM, $n = 12-16$, ** $P < 0.05$). C, pH, (D) urea, (E) creatinine (limit of detection $18 \mu\text{mol/L}$) measured in whole blood by the iSTAT point-of-care analyzer. F, Core temperature, measured by rectal probe in unconscious sham WT and GFRP OE mice and 6 and 24 h after CLP (mean \pm SEM, $n = 6-8$, ** $P < 0.05$ compared with sham).

after CLP. However, OE mice displayed increased GFRP protein expression at each time point studied, compared with WT littermates (Fig. 4E).

DISCUSSION

The salient finding from this study is that conditional overexpression of GFRP can curtail the increases in systemic BH_4 , cardiac NO, cardiovascular dysfunction, metabolic acidosis, and renal dysfunction observed in a CLP mouse model of sepsis. These results indicate that changes in the GFRP:GCH1 ratio contribute to the cardiovascular and metabolic dysfunction observed in septic shock (Fig. 5).

We have previously shown that GFRP overexpression attenuates the increase in BH_4 and NO arising in response to a proinflammatory stimulus *in vitro* (20). In the present study,

we wished to determine the physiological significance of this finding. While mouse models of sepsis have come under close scrutiny, Osuchowski et al. (31) have argued that mice sufficiently emulate numerous pathophysiological alterations produced by sepsis and can serve as an experimental platform for answering clinically relevant questions.

We hypothesized that overexpression of GFRP would maintain the sensitivity of GCH1 to feedback inhibition, limit BH_4 bioavailability, and reduce pathological NO production, in a clinically relevant model of septic shock in which NO production is increased (32, 33).

We validated the specificity and efficiency of Cre-mediated recombination by crossing dormant GFRP transgenic mice with Cre recombinase mice under the control of an $\alpha\text{SM-Cre}$ promoter and subsequently characterized the cardiovascular and metabolic phenotype under naive and septic conditions.

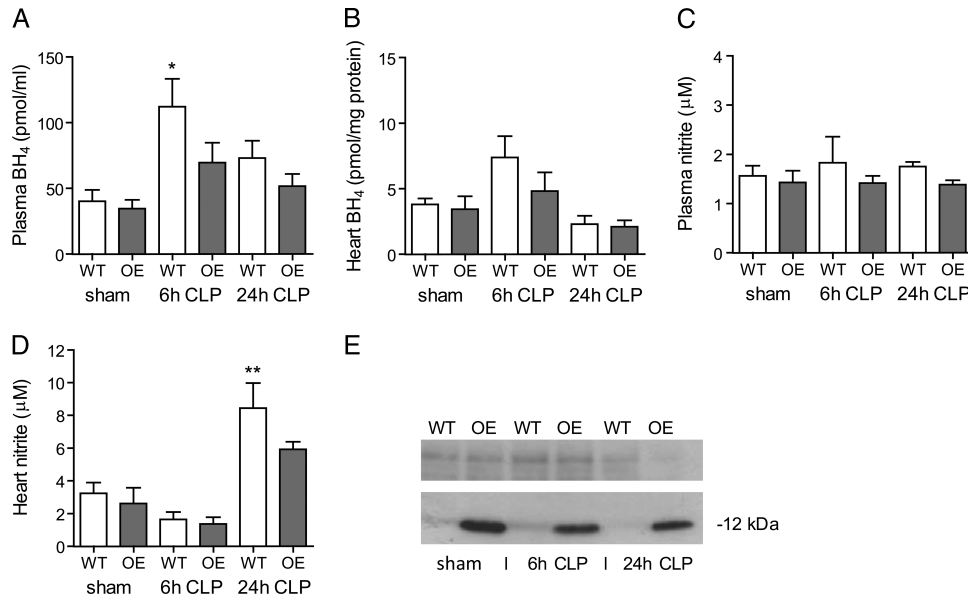


FIG. 4. **BH₄ and nitrite measurement in septic mice.** A, Plasma and (B) heart BH₄ measured by HPLC in sham and CLP-treated (6 and 24 h) WT and GFRP OE mice (n = 4–6, mean ± SEM, *P < 0.05 compared with sham). Fluorometric analysis of (C) plasma and (D) heart nitrite levels in sham and CLP-treated (6 and 24 h) WT and GFRP OE mice (n = 3–5, mean ± SD, **P < 0.01 compared with sham). E, Immunoblotting with mouse GFRP monoclonal antibody to detect overexpression of GFRP protein identified a specific 12-kd band in lysates from heart tissue from sham animals and 6 and 24 h following CLP. The stained membrane used as loading control.

Consistent with published reports, we observed excision of the Stop cassette and marked overexpression of GFRP in the expected tissues, heart, and skeletal muscle (26).

Basal GFRP expression was very low in WT mice in all tissues studied, with the exception of the liver, consistent with previous reports (27). Despite marked GFRP overexpression in certain tissues, we did not observe any statistically significant differences in basal BH₄ levels between WT and GFRP OE mice, a finding inconsistent with a previous study (27). The

reason for this discrepancy may be associated with the method used to detect BH₄ levels or differences in the promoter used to drive Cre expression and downstream GFRP expression profile.

Nevertheless, our observed lack of effect of GFRP overexpression on basal BH₄ and nitrite levels is consistent with previous observations in endothelial cells (20) and in GCH1-GFRP-overexpressing fibroblasts (34). This supports the notion that under basal conditions BH₄ is not present in high-enough concentrations to elicit end-product feedback inhibition via the GCH1-GFRP complex and therefore maintains sufficient BH₄ for the constitutively expressed NOS isoforms (endothelial and neuronal NOS). This is further supported by our observation that both GFRP OE and WT mice display similar baseline cardiovascular hemodynamics.

In contrast to baseline hemodynamics and biochemistry, when the system was perturbed by an inflammatory stimulus (CLP), we observed clear differences in the cardiovascular and biochemical profile between GFRP OE and WT mice.

It is well established that a proinflammatory-induced rise in NO supports the host defense response to invading pathogens, but that overproduction of vascular NO is associated with the cardiovascular derangements that occur in septic shock (2, 3, 35). The ability of the body to generate such large amounts of NO arises as a consequence of changes in the expression of NOS isoforms, in particular iNOS, which in turn contributes toward the observed cardiovascular dysfunction (32, 36). However, raised expression/activity of other NOS isoforms has also been described in sepsis (37). Irrespective of which NOS isoform is upregulated under inflammatory conditions, all newly translated NOS isoforms require BH₄ for full activity and dimer stabilization (4, 38).

In WT mice, we observed temporal changes in BH₄ levels, consistent with proinflammatory stimulation of GCH1 and

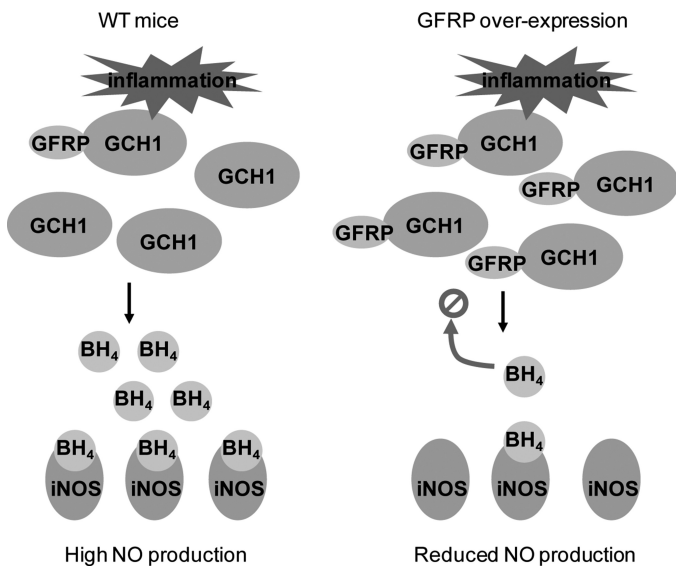


FIG. 5. **Effect of GFRP overexpression during septic shock.** Proinflammatory conditions upregulate GCH1 and downregulate GFRP, maximizing BH₄ availability for iNOS. Excessive NO generation ensues, resulting in hypotension and cardiac and microcirculatory dysfunction. Overexpression of GFRP ensures GCH1 activity is tightly regulated through feedback inhibition by accumulating BH₄, resulting in reduced cofactor availability for iNOS activity and limited NO generation. This results in the attenuation of pathology following induction of septic shock.

with the clinical observation that urinary neopterin (a product of GCH1 activity) is raised in septic patients (39). We also observed a significant rise in nitrite at 24 h in cardiac tissue, consistent with clinical observations that nitrite levels are raised in septic patients (40).

Furthermore, in response to CLP, all mice displayed tachycardia, reduced cardiac output, and arteriolar and microvascular dysfunction compared with their paired time-matched control values and consistent with changes observed clinically.

Despite an initial tachycardic response in all septic mice, the heart rate gradually decreased over time in WT mice, correlating with maximal NO levels in cardiac tissue 24 h after CLP. In contrast, heart rate remained elevated, and cardiac nitrite levels were attenuated in GFRP OE mice. It is known that overproduction of NO in the myocardium contributes to impaired contractility (41), and our findings are consistent with the high degree of GFRP overexpression achieved in the heart. Reduced GCH1 activity and subsequent BH₄ deficiency have been shown to reduce contractile function (42) but also increase cardiac sensitivity to catecholamines (43), which are elevated during sepsis; this likely accounts for the elevated HR exhibited by GFRP OE mice following CLP.

It is becoming increasingly apparent that sepsis is a disease of the microcirculation, and microcirculatory disturbances correlate with poorer patient outcome (44). We therefore used a laser speckle contrast imaging system to visualize and quantify microcirculatory perfusion in the mesenteric bed.

We observed a striking reduction in mesenteric perfusion in all CLP-treated mice, despite a relatively modest decrease in systolic blood pressure. These data suggest that macrovascular hemodynamic stability is maintained at the expense of the microvascular circulation, but although peripheral constriction/thrombosis contributes to sustain mean arterial blood pressure, it also results in insufficient organ perfusion in septic shock.

Consistent with reduced mesenteric perfusion, all mice exhibited evidence of metabolic acidosis and raised urea levels 24 h after CLP. Although we did not detect significant differences in microcirculatory mesenteric perfusion between GFRP OE and WT mice, there was evidence of a worsened biochemical phenotype in WT mice as quantified by marked acidosis and renal dysfunction. This suggests that whilst mesenteric perfusion was equally impaired, global perfusion was improved in GFRP OE mice. Indeed, GFRP overexpression was pronounced in skeletal muscle, a tissue in which NO overproduction has been implicated in contributing to pathology (45).

Our study confirms that in a murine model of septic shock, GCH1 activity is increased (evidenced by elevated BH₄), and GFRP production is decreased (evidenced by reduced protein expression), and this is associated with changes in NO and cardiovascular derangements. The observed reduction in GFRP protein expression following CLP is consistent with previous reports *in vitro* (18). However, studies in vascular smooth muscle cells have shown that while GFRP expression does increase following proinflammatory stimulation, the magnitude of the increase is markedly lower than that of GCH1 (19). In either case, the ratio of GCH1:GFRP is increased under inflammatory conditions, rendering GCH1 less sensitive to feedback inhibition by BH₄, in turn leading to enhanced NO production.

The present study, coupled with our previous *in vitro* model (20), demonstrates that manipulation of the GCH1:GFRP ratio, through GFRP overexpression, allows tighter regulation of GCH1 under inflammatory conditions, as evidenced by reduced BH₄ and NO, and an attenuation of the pathological changes observed following CLP-induced sepsis. We further demonstrate that microcirculatory perfusion is substantially impaired despite more modest changes in macrocirculatory hemodynamics, highlighting the importance of quantifying microcirculatory disturbances in septic shock.

These findings suggest that agents that mimic the allosteric regulation of the GCH1-GFRP axis could potentially have therapeutic value, regulating BH₄ biosynthesis during the development of septic shock.

CONCLUSIONS

We have shown that modification of the GFRP:GCH1 ratio regulates BH₄ and NO biosynthesis and cardiovascular function, identifying GFRP-GCH1 interactions as a key regulator of the cardiovascular system during septic shock.

ACKNOWLEDGMENT

The authors thank Dr Eileen McNeill, Oxford University, for access and training in using the BH₄ detector.

REFERENCES

- Dunser MW, Ruokonen E, Pettila V, et al.: Association of arterial blood pressure and vasopressor load with septic shock mortality: a post hoc analysis of a multicenter trial. *Crit Care* 13(6):R181, 2009.
- Trzeciak S, Cinel I, Phillip DR, et al.: Resuscitating the microcirculation in sepsis: the central role of nitric oxide, emerging concepts for novel therapies, and challenges for clinical trials. *Acad Emerg Med* 15(5):399–413, 2008.
- Cauwels A, Brouckaert P: Nitrite regulation of shock. *Cardiovasc Res* 89(3):553–559, 2011.
- Tayeh MA, Marletta MA: Macrophage oxidation of L-arginine to nitric oxide, nitrite, and nitrate. Tetrahydrobiopterin is required as a cofactor. *J Biol Chem* 264(33):19654–19658, 1989.
- Nichol CA, Lee CL, Edelstein MP, et al.: Biosynthesis of tetrahydrobiopterin by de novo and salvage pathways in adrenal medulla extracts, mammalian cell cultures, and rat brain *in vivo*. *Proc Natl Acad Sci U S A* 80(6):1546–1550, 1983.
- Stevens LM, Fortier S, Aubin MC, et al.: Effect of tetrahydrobiopterin on selective endothelial dysfunction of epicardial porcine coronary arteries induced by cardiopulmonary bypass. *Eur J Cardiothorac Surg* 30(3):464–471, 2006.
- Du YH, Guan YY, Alp NJ, et al.: Endothelium-specific GTP cyclohydrolase I overexpression attenuates blood pressure progression in salt-sensitive low-renin hypertension. *Circulation* 117(8):1045–1054, 2008.
- Cosentino F, Hurlimann D, Delli GC, et al.: Chronic treatment with tetrahydrobiopterin reverses endothelial dysfunction and oxidative stress in hypercholesterolaemia. *Heart* 94(4):487–492, 2008.
- Starr A, Hussein D, Nandi M: The regulation of vascular tetrahydrobiopterin bioavailability. *Vascul Pharmacol* 58(3):219–230, 2013.
- Kaspers B, Gutlich M, Witter K, et al.: Coordinate induction of tetrahydrobiopterin synthesis and nitric oxide synthase activity in chicken macrophages: upregulation of GTP-cyclohydrolase I activity. *Comp Biochem Physiol B Biochem Mol Biol* 117(2):209–215, 1997.
- Katusic ZS, Stelter A, Milstien S: Cytokines stimulate GTP cyclohydrolase I gene expression in cultured human umbilical vein endothelial cells. *Arterioscler Thromb Vasc Biol* 18(1):27–32, 1998.
- Yoshida M, Nakanishi N, Wang X, et al.: Exogenous biopterins requirement for iNOS function in vascular smooth muscle cells. *J Cardiovasc Pharmacol* 42(2):197–203, 2003.
- Bahrami S, Fitzal F, Peichl G, et al.: Protection against endotoxemia in rats by a novel tetrahydrobiopterin analogue. *Shock* 13(5):386–391, 2000.
- Li HY, Yao YM, Shi ZG, et al.: Effect of 2,4-diamino-6-hydroxy-pyrimidine on postburn *Staphylococcus aureus* sepsis in rats. *Crit Care Med* 30(11):2520–2527, 2002.
- Bendall JK, Alp NJ, Warrick N, et al.: Stoichiometric relationships between endothelial tetrahydrobiopterin, endothelial NO synthase (eNOS) activity, and

- eNOS coupling *in vivo*: insights from transgenic mice with endothelial-targeted GTP cyclohydrolase 1 and eNOS overexpression. *Circ Res* 97(9):864–871, 2005.
16. Harada T, Kagamiyama H, Hatakeyama K: Feedback regulation mechanisms for the control of GTP cyclohydrolase I activity. *Science* 260(5113):1507–1510, 1993.
 17. Maita N, Hatakeyama K, Okada K, et al.: Structural basis of biopterin-induced inhibition of GTP cyclohydrolase I by GFRP, its feedback regulatory protein. *J Biol Chem* 279(49):51534–51540, 2004.
 18. Werner ER, Bahrami S, Heller R, et al.: Bacterial lipopolysaccharide down-regulates expression of GTP cyclohydrolase I feedback regulatory protein. *J Biol Chem* 277(12):10129–10133, 2002.
 19. Xie L, Smith JA, Gross SS: GTP cyclohydrolase I inhibition by the prototypic inhibitor 2,4-diamino-6-hydroxypyrimidine. Mechanisms and unanticipated role of GTP cyclohydrolase I feedback regulatory protein. *J Biol Chem* 273(33):21091–21098, 1998.
 20. Nandi M, Kelly P, Vallance P, et al.: Over-expression of GTP-cyclohydrolase I feedback regulatory protein attenuates LPS and cytokine-stimulated nitric oxide production. *Vasc Med* 13(1):29–36, 2008.
 21. Nandi M, Kelly P, Torondel B, et al.: Genetic and pharmacological inhibition of dimethylarginine dimethylaminohydrolase 1 is protective in endotoxemic shock. *Arterioscler Thromb Vasc Biol* 32(11):2589–2597, 2012.
 22. Kilkeny C, Browne WJ, Cuthill IC, et al.: Improving bioscience research reporting: the ARRIVE guidelines for reporting animal research. *Osteoarthritis Cartilage* 20(4):256–260, 2012.
 23. Rittirsch D, Huber-Lang MS, Flierl MA, et al.: Immunodesign of experimental sepsis by cecal ligation and puncture. *Nat Protoc* 4(1):31–36, 2009.
 24. Howells DW, Smith I, Hyland K: Estimation of tetrahydrobiopterin and other pterins in cerebrospinal fluid using reversed-phase high-performance liquid chromatography with electrochemical and fluorescence detection. *J Chromatogr* 381(2):285–294, 1986.
 25. Brambilla DJ, Matsumoto AM, Araujo AB, et al.: The effect of diurnal variation on clinical measurement of serum testosterone and other sex hormone levels in men. *J Clin Endocrinol Metab* 94(3):907–913, 2009.
 26. Maruyama T, Hatakeyama S, Miwa T, et al.: Human smooth muscle alpha-actin promoter drives Cre recombinase expression in the cranial suture in addition to smooth muscle cell. *Biosci Biotechnol Biochem* 71(4):1103–1106, 2007.
 27. Pathak R, Pawar SA, Fu Q, et al.: Characterization of transgenic GFRP knock-in mice: implications for tetrahydrobiopterin in modulation of normal tissue radiation responses. *Antioxid Redox Signal* 20(9):1436–1446, 2014.
 28. Takala J: Determinants of splanchnic blood flow. *Br J Anaesth* 77(1):50–58, 1996.
 29. Van der Crabben SN, Blumer RM, Stegenga ME, et al.: Early endotoxemia increases peripheral and hepatic insulin sensitivity in healthy humans. *J Clin Endocrinol Metab* 94(2):463–468, 2009.
 30. Lang CH, Dobrescu C: Sepsis-induced increases in glucose uptake by macrophage-rich tissues persist during hypoglycemia. *Metabolism* 40(6):585–593, 1991.
 31. Osuchowski MF, Remick DG, Lederer JA, et al.: Abandon the mouse research ship? Not just yet! *Shock* 41(6):463–475, 2014.
 32. Hollenberg SM, Broussard M, Osman J, et al.: Increased microvascular reactivity and improved mortality in septic mice lacking inducible nitric oxide synthase. *Circ Res* 86(7):774–778, 2000.
 33. Park JH, Na HJ, Kwon YG, et al.: Nitric oxide (NO) pretreatment increases cytokine-induced NO production in cultured rat hepatocytes by suppressing GTP cyclohydrolase I feedback inhibitory protein level and promoting inducible NO synthase dimerization. *J Biol Chem* 277(49):47073–47079, 2002.
 34. Tatham AL, Crabtree MJ, Warrick N, et al.: GTP cyclohydrolase I expression, protein, and activity determine intracellular tetrahydrobiopterin levels, independent of GTP cyclohydrolase feedback regulatory protein expression. *J Biol Chem* 284(20):13660–13668, 2009.
 35. Bateman RM, Sharpe MD, Ellis CG: Bench-to bedside review: microvascular dysfunction in sepsis—hemodynamics, oxygen transport, and nitric oxide. *Crit Care* 7(5):359–373, 2003.
 36. Chauhan SD, Seggara G, Vo PA, et al.: Protection against lipopolysaccharide-induced endothelial dysfunction in resistance and conduit vasculature of iNOS knockout mice. *FASEB J* 17(6):773–775, 2003.
 37. Araujo AV, Ferezin CZ, Pereira AC, et al.: Augmented nitric oxide production and up-regulation of endothelial nitric oxide synthase during cecal ligation and perforation. *Nitric Oxide* 27(1):59–66, 2012.
 38. Panda K, Rosenfeld RJ, Ghosh S, et al.: Distinct dimer interaction and regulation in nitric-oxide synthase types I, II, and III. *J Biol Chem* 277(34):31020–31030, 2002.
 39. Baydar T, Yuksel O, Sahin TT, et al.: Neopterin as a prognostic biomarker in intensive care unit patients. *J Crit Care* 24(3):318–321, 2009.
 40. Ochoa JB, Udekwo AO, Billiar TR, et al.: Nitrogen oxide levels in patients after trauma and during sepsis. *Ann Surg* 214(5):621–626, 1991.
 41. Preiser JC, Zhang H, Vray B, et al.: Time course of inducible nitric oxide synthase activity following endotoxin administration in dogs. *Nitric Oxide* 5(2):208–211, 2001.
 42. Ceylan-Isik AF, Guo KK, Carlson EC, et al.: Metallothionein abrogates GTP cyclohydrolase I inhibition-induced cardiac contractile and morphological defects: role of mitochondrial biogenesis. *Hypertension* 53(6):1023–1031, 2009.
 43. Adlam D, Herring N, Douglas G, et al.: Regulation of beta-adrenergic control of heart rate by GTP-cyclohydrolase I (GCH1) and tetrahydrobiopterin. *Cardiovasc Res* 93(4):694–701, 2012.
 44. De Backer D, Creteur J, Preiser JC, et al.: Microvascular blood flow is altered in patients with sepsis. *Am J Respir Crit Care* 166(1):98–104, 2002.
 45. Lidington D, Li F, Tysl K: Deletion of neuronal NOS prevents impaired vasodilation in septic mouse skeletal muscle. *Cardiovasc Res* 74(1):151–158, 2007.

